Contribution from the Kenan Laboratories of Chemistry, The University of North Carolina, Chapel Hill, North Carolina 27599-3290, and Department of Chemistry, Stanford University, Stanford, California 94305

Electrochemical Olefin Epoxidation with Manganese *meso*-Tetraphenylporphyrin Catalyst and Hydrogen Peroxide Generation at Polymer-Coated Electrodes

Hiroshi Nishihara,[†] K. Pressprich,[†] Royce W. Murray,*[,†] and James P. Collman[‡]

Received December 2, 1988

An electrocatalytic reaction for olefin epoxidation is presented. Hydrogen peroxide is generated electrochemically by reduction of dioxygen in methylene chloride solvent containing benzoic acid as proton source, [Mn(TPP)Cl] as catalyst, 1-methylimidazole as axial base, and olefin as substrate. The glassy-carbon electrode is coated with a 20–80-nm film of poly-$[Ru(vbpy)_3]^{2+}$, which has high permeability to dioxygen and very low permeability to porphyrin. The polymer film prevents electrochemical reduction of the high-valent metal oxo porphyrin [Mn(=O)TPP]. At high concentrations of olefin and porphyrin, the electrocatalytic reaction runs at nearly 100% current efficiency for production of cyclooctene oxide. At lower porphyrin concentrations, catalyst degradation occurs, and at low olefin concentrations, an apparent catalase-like side reaction lowers the yield of epoxide. The porphyrin degradation but not the catalase-like side reaction was lessened by using the protected porphyrins [Mn(TMP)Cl] and [Mn(T-F_5PP)Cl].

Achieving catalytic, stereospecific, and regioselective olefin epoxidation with synthetic metalloporphyrin models of cytochrome P-450[1] is a topic of continuing research interest. High-valent oxo porphyrins, the active olefin oxidant, have been generated in diverse ways, with direct oxygen atom transfer agents such as iodosobenzenes,[2] hypochlorate,[3,4] *N*,*N*-dimethylaniline *N*-oxides,[5] percarboxylic acids,[6,7] hydroperoxides,[6,8] and oxaziridines,[9] with reduced dioxygen species,[10] and with dioxygen plus reductant.[11,12a] The pathways relying on dioxygen are especially intriguing from the viewpoints of biomimesis and practical utilization of molecular oxygen.

We have used electrochemical reactions to produce high-valent oxo porphyrins. Electrochemical potential control can supply reducing equivalents in a more easily adjustable manner than can reaction mixtures containing chemical reductants. We have also demonstrated electrochemical mimesis of the P-450 catalytic cycle,[12a] by means of electrocatalytic reduction of [Mn(TPP)Cl] (TPP = *meso*-tetraphenylporphyrin) at a carbon electrode in a CH_2Cl_2 solution of olefin, 1-methylimidazole, O_2, and acid anhydride. Conditions were chosen in which the initial electroreduction of porphyrin was followed by O_2 binding, passage of a second electron, and heterolysis of a $[Mn^{III}(TPP)O_2]^{2-}$ complex by the acid anhydride.

This paper describes a new electrocatalytic approach to epoxidation that generates H_2O_2 by electroreducing O_2, the H_2O_2 then reacting with porphyrin to generate the oxo porphyrin (Scheme I). The reaction involves CH_2Cl_2 solutions of olefin, [Mn(TPP)Cl], 1-methylimidazole, O_2, benzoic acid as proton source, and a polymer-coated electrode. Reduction of the precursor porphyrin or of the active oxo porphyrin[3d,12b,13] oxidant by the electrode is circumvented by the polymer electrode coating which is permeable[14] to O_2 but acts as a transport barrier to the more bulky porphyrins. The electrode coating used is an electropolymerized film[15] of poly-$[Ru(vbpy)_3]^{2+}$. Scheme I achieves great efficiency because unproductive reduction of oxo porphyrin is avoided and because the current (electron supply) is not limited by the diffusion of porphyrin catalyst at a low concentration.[12] We also report electrocatalysis with the hindered porphyrins [Mn(TMP)Cl] (TMP = *meso*-tetramesitylporphyrin) and [Mn(TF_5PP)Cl] (TF_5PP = *meso*-tetrakis(pentafluorophenyl)-porphyrin).

Olefin epoxidation based on [Mn(TPP)Cl]–H_2O_2 reactions, and direct addition of H_2O_2, was earlier reported by Mansuy,[8] who noticed some loss of [Mn(TPP)Cl] catalyst even when the H_2O_2 was added slowly. The porphyrin stability observed in the present studies shows that chemical degradation effects of H_2O_2 can be greatly lessened by the more precise electrochemical control of the oxidant supply.

Scheme I

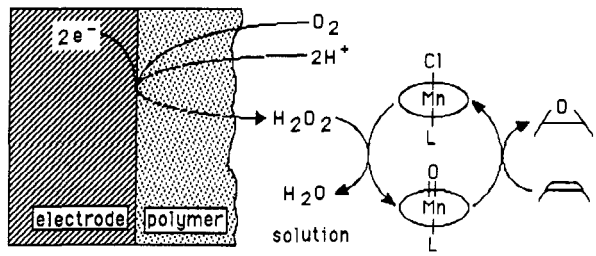

(1) Recent reviews: (a) Ortiz de Montellano, P. R. *Acc. Chem. Res.* **1987**, *20*, 289. (b) Dawson, J. H.; Sono, M. *Chem. Rev.* **1987**, *87*, 1255. (c) McMurray, T. J.; Groves, J. T. In *Cytochrome P-450*; oritze de Montellano, P. R., Ed.; Plenum: New York, 1986; Chapter 1. (d) Holm, R. H. *Chem. Rev.* **1987**, *87*, 1401.

(2) (a) Groves, J. T.; Nemo, T. E.; Myers, R. S. *J. Am. Chem. Soc.* **1979**, *101*, 1032. (b) Groves, J. T.; Kruper, W. J., Jr. *Ibid.* **1979**, *101*, 7613. (c) Groves, J. T.; Kruper, W. J., Jr.; Nemo, T. E.; Myers, R. S. *J. Mol. Catal.* **1980**, *7*, 169. (d) Groves, J. T.; Kruper, W. J., Jr.; Haushalter, R. C.; Butler, W. M. *Inorg. Chem.* **1982**, *21*, 1363. (e) Groves, J. T.; Nemo, T. E. *J. Am. Chem. Soc.* **1983**, *105*, 5786. (f) Lindsay-Smith, J. R.; Steath, P. R. *J. Chem. Soc., Perkin Trans. 2* **1982**, 1009. (g) Schardt, B. C.; Hollander, F. J.; Hill, C. L. *J. Am. Chem. Soc.* **1982**, *104*, 3964. (h) Smegal, J. A.; Hill, C. L. *Ibid.* **1983**, *105*, 2920. (i) Smegal, J. A.; Schardt, B. C.; Hill, C. L. *Ibid.* **1983**, *105*, 3510. (j) Traylor, P. S.; Dolphin, D.; Traylor, T. G. *J. Chem. Soc., Chem. Commun.* **1984**, 279. (k) Traylor, T. G.; Marsters, J. C., Jr.; Nakano, T.; Dunlap, B. E. *J. Am. Chem. Soc.* **1985**, *107*, 5537. (l) Collman, J. P.; Kodadek, T.; Raybuck, S. A.; Brauman, J. I.; Papazian, L. M. *Ibid.* **1985**, *107*, 4343.

(3) (a) Guilmet, E.; Meunier, B. *Tetrahedron Lett.* **1980**, *21*, 4449. (b) Guilmet, E.; Meunier, B. *Nouv. J. Chim.* **1982**, *6*, 551. (c) Guilmet, E.; Meunier, B. *Tetrahedron Lett.* **1982**, *23*, 2449. (d) Bortolini, O.; Meunier, B. J. *J. Chem. Soc., Chem. Commun.* **1983**, 1364. (e) Guilmet, E.; Meunier, B. *J. Mol. Catal.* **1984**, *23*, 115. (f) Meunier, B.; Guilmet, E.; DeCarvallo, M. E.; Poibanc, R. *J. Am. Chem. Soc.* **1984**, *106*, 6668. (g) Collman, J. P.; Kodadek, T.; Raybuck, S. A.; Meunier, B. *Proc. Natl. Acad. U.S.A.* **1983**, *80*, 7039.

(4) (a) Collman, J. P.; Brauman, J. I.; Meunier, B.; Raybuck, S. A.; Kodadek, T. *Proc. Natl. Acad. Sci. U.S.A.* **1984**, *81*, 3245. (b) Collman, J. P.; Brauman, J. I.; Meunier, B.; Hayashi, T.; Kodadek, T.; Raybuck, S. A. *J. Am. Chem. Soc.* **1985**, *107*, 2000.

(5) (a) Nee, M. W.; Bruice, T. C. *J. Am. Chem. Soc.* **1982**, *104*, 6123. (b) Powell, M. F.; Pai, E. F.; Bruice, T. C. *Ibid.* **1984**, *106*, 3277. (c) Dicken, C. M.; Woon, T. C.; Bruice, T. C. *Ibid.* **1986**, *108*, 1636.

(6) (a) Yuan, L.-C.; Bruice, T. C. *Inorg. Chem.* **1985**, *24*, 987. (b) Lee, W. A.; Bruice, T. C. *Ibid.* **1986**, *25*, 131. (c) Yuan, L.-C.; Bruice, T. C. *J. Am. Chem. Soc.* **1986**, *108*, 1643.

(7) (a) Groves, J. T.; Haushalter, R. C.; Nakamura, M.; Nemo, T. E.; Evans, B. J. *J. Am. Chem. Soc.* **1981**, *103*, 2884. (b) Traylor, T. G.; Lee, W. A.; Stynes, D. V. *Ibid.* **1984**, *106*, 755.

(8) Renaud, J.-P.; Battioni, P.; Bartoli, J. F.; Mansuy, D. *J. Chem. Soc., Chem. Commun.* **1985**, 888.

(9) (a) Yuan, L.-C.; Bruice, T. C. *J. Am. Chem. Soc.* **1985**, *107*, 512. (b) Lee, W. A.; Bruice, T. C. *Ibid.* **1985**, *107*, 513.

[†] The University of North Carolina.
[‡] Stanford University.

0020-1669/90/1329-1000$02.50/0

Experimental Section

Chemicals. Spectroquality grade acetonitrile and dichloromethane (Burdick and Jackson) were dried with 4-Å molecular sieves. Tetra-*n*-butylammonium perchlorate (Bu_4NClO_4) was prepared from tetra-*n*-butylammonium bromide and perchloric acid and recrystallized three times from ethyl acetate. 1-Methylimidazole was distilled twice under reduced pressure. *trans*-2-Octene oxide was prepared from *trans*-2-octene and *m*-chloroperbenzoic acid and distilled twice. $[Ru(vbpy)_3](ClO_4)_2$ (vbpy = 4-methyl-4′-vinylbipyridine), prepared according to the literature,[16] was purified by column chromatography (Al_2O_3) and three recrystallizations from ethyl acetate–methanol. The concentration of perbenzoic acid solution in chloroform prepared by a published method[17] was determined by iodometry. [Mn(TPP)Cl], [Mn(TMP)Cl], [Mn(T-F_5PP)Cl], and cyclooctene oxide were previously prepared in this laboratory.[12b] Other reagents were of high-purity commercial reagent grade.

Instruments. Cyclic voltammetry experiments were performed with a potentiostat and wave form generator of local construction, rotating-disk experiments were performed with a PAR 173 potentiostat and a Pine Instruments Model ASR-2 variable-speed rotator, vis–UV spectrophotometric studies were performed with a Hewlett-Packard 8450A spectrometer, and GC electrode epoxide analysis was performed with a Shimadzu GC-14A analyzer with a OV-101/chrom W-HP column (Alltech Applied Science Laboratories), FID detector, and Shimadzu CR4A data processor.

Electrochemical Experiments. Teflon-shrouded glassy-carbon (GC, Atomergic) electrodes were polished with 0.25-μm alumina (Buehler) and thoroughly washed with distilled water, acetone, and acetonitrile. Platinum electrodes were polished with 0.3-μm diamond paste (Buehler), washed with distilled water, cleaned by potential cycling between +1.1 and −0.22 V vs SSCE in 0.5 M H_2SO_4 until sharp hydrogen adsorption waves developed, and washed with distilled water, acetone, and acetonitrile. Electrochemical cells had three compartments, for working, Pt counter, and Ag/Ag^+ (0.01 M $AgClO_4$ in 0.1 M Bu_4NClO_4–CH_3CN) reference electrodes.

Poly-$[Ru(vbpy)_3](ClO_4)_2$ films were formed by electropolymerization of 0.1–0.5 mM monomer complex in deaerated 0.1 M Bu_4NClO_4–CH_3CN by consecutive potential scans between −1.25 and −1.95 V vs Ag/Ag^+. Film thickness was characterized by the quantity of electroactive sites in the film, Γ_T (mol/cm^2), measured from the charge under the cyclic voltammogram of the Ru(III/II) couple in 0.1 M Bu_4NClO_4–CH_3CN.

Precisely reproducible transport conditions were obtained in controlled-potential epoxidation electrolysis by using a rotated-disk working electrode, at 400–1600 rpm in a CH_2Cl_2 solution exposed to the air. Fresh CH_2Cl_2 was added periodically to replenish evaporated solvent. Typical epoxidation electrolysis solutions contained 0.1 M Bu_4NClO_4 electrolyte, 0.1 M benzoic acid, 0.04 M 1-methylimidazole, olefin, [Mn(TPP)Cl], and decane as internal standard for the GC analysis of epoxide yield.

Analysis of H_2O_2 Yields. Hydrogen peroxide formed by electroreduction of O_2 in CH_2Cl_2 was extracted with three small portions of distilled water that were combined and added to 1 mL of $Ti(SO_4)_2$ test solution[18] and enough distilled water to make a total volume of 10 mL. The solution was filtered, and its absorbance at 432 nm was used for the colorimetric analysis. Electrolyses that tested for hydrogen peroxide production lasted 10–30 min, and the solutions were the same as above excepting olefin, decane, and [Mn(TPP)Cl] were absent.

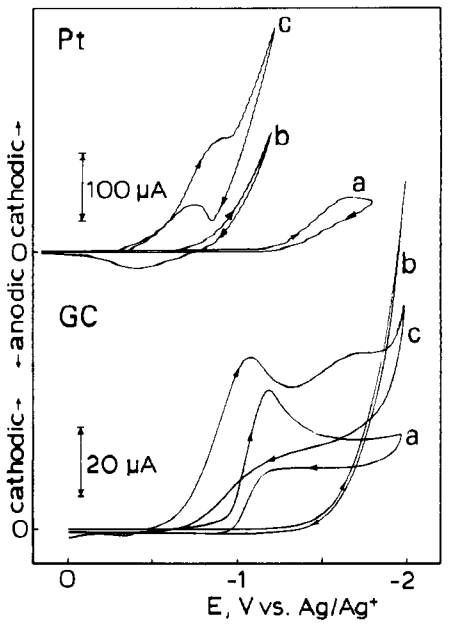

Figure 1. Cyclic voltammograms recorded at 0.1 V/s at a 0.091 cm^2 Pt (upper curves) and a 0.053-cm^2 GC electrode in 0.1 M Bu_4NClO_4–CH_2Cl_2: curves a, in air; curves b, with 0.1 M benzoic acid under Ar; curves c, with 0.1 M benzoic acid in air.

Table I. H_2O_2 Yield by Electroreduction of O_2 in Bu_4NClO_4–CH_2Cl_2 with 0.1 M Benzoic Acid

		H_2O_2 yield, %[a]	
electrode	potential, V vs Ag/Ag^+	naked electrode	polymer-coated electrode[b]
Pt	−0.8	19	
	−0.9	12	
	−1.1	9	8[c]
GC	−1.0		97[d]
	−1.1	73	100[c]
	−1.3	81	99, 100[d]

[a] Faradaic efficiency assuming 2e generate 1 H_2O_2. [b] Polymer = poly-$[Ru(vbpy)_3]^{2+}$. [c] 0.2 M 1-methylimidazole. [d] 0.04 M 1-methylimidazole.

Results and Discussion

Electrochemical Reduction of O_2 at Naked Electrodes in Methylene Chloride. While the quasi-reversible reduction of O_2 in the aprotic solvents DMF and Me_2SO is well-known,[19] it is not in CH_2Cl_2, and it was necessary to work out the details of producing H_2O_2 by O_2 reduction in this solvent. The cyclic voltammetric reduction of O_2 in CH_2Cl_2 with no added proton source (curves a, Figure 1) is chemically irreversible at both Pt and GC electrodes at a scan rate of 0.1 V/s. Faster, 1 V/s, potential scans at GC electrodes produce a reoxidation current peak that is 58% as large as the reduction peak. This behavior indicates that the chemical decay of the initial superoxide reduction product, which is reported[20] by reaction with CH_2Cl_2 to yield formaldehyde, Cl^-, and O_2, is relatively slow.

H_2O_2 production from O_2 reduction is facilitated when a proton source is available, and curves c, Figure 1, show that adding

(10) (a) Groves, J. T.; Watanabe, Y.; McMurry, T. J. *J. Am. Chem. Soc.* **1983**, *105*, 4489. (b) Khenkin, A. M.; Shteinman, A. A. *J. Chem. Soc., Chem. Commun.* **1984**, 1219. (c) Burstyn, J. N.; Roe, J. A.; Mikstal, A. R.; Shaevitz, B. A.; Lang, G.; Valentine, J. S. *J. Am. Chem. Soc.* **1988**, *110*, 1382. (d) VanAtta, R. B.; Strouse, C. E.; Hanson, L. K.; Valentine, J. S. *J. Am. Chem. Soc.* **1987**, *109*, 1425.

(11) (a) Tabushi, I.; Koga, N. *J. Am. Chem. Soc.* **1979**, *101*, 6456. (b) Tabushi, I.; Yazaki, A. *Ibid.* **1981**, *103*, 7371. (c) Tabushi, I.; Morimitsu, K. *Ibid.* **1984**, *106*, 6871. (d) Tabushi, I.; Kodera, M.; Yokoyama, M. *Ibid.* **1985**, *107*, 4466. (e) Tabushi, I.; Kodera, M. *Ibid.* **1986**, *108*, 1101. (f) Mansuy, D.; Fontecave, M.; Bartoli, J.-F. *J. Chem. Soc., Chem. Commun.* **1983**, 253. (g) Groves, J. T.; Quinn, R. *J. Am. Chem. Soc.* **1985**, *107*, 5790. (h) Fontecave, M.; Mansuy, D. *Tetrahedron* **1984**, *40*, 2847. (i) Battioni, P.; Bartori, J. F.; Leduc, P.; Fontecave, M.; Mansuy, D. *J. Chem. Soc., Chem. Commun.* **1987**, 791. (j) Moisy, P.; Bedioui, F.; Robin, Y.; Devynck, J. *J. Electroanal. Chem.* **1988**, *250*, 191.

(12) (a) Creager, S. E.; Raybuck, S. A.; Murray, R. W. *J. Am. Chem. Soc.* **1986**, *108*, 4225. (b) Creager, S. E.; Murray, R. W. *Inorg. Chem.* **1987**, *26*, 2612.

(13) Carnier, N.; Harriman, A.; Porter, G. *J. Chem. Soc., Dalton Trans.* **1982**, 931.

(14) (a) Ikeda, T.; Schmehl, R.; Denisevich, P.; Willman, K.; Murray, R. W. *J. Am. Chem. Soc.* **1982**, *104*, 2683. (b) Ewing, A. G.; Feldman, B. J.; Murray, R. W. *J. Electroanal. Chem.* **1984**, *172*, 145.

(15) Denisevich, P.; Abruna, H. D.; Leidner, C. R.; Meyer, T. J.; Murray, R. W. *Inorg. Chem.* **1982**, *21*, 2153.

(16) Abruna, H. D.; Denisevich, P.; Umana, M.; Meyer, T. J.; Murray, R. W. *J. Am. Chem. Soc.* **1981**, *103*, 1.

(17) (a) Ogata, Y.; Sawaki, Y. *Tetrahedron* **1967**, *23*, 3327. (b) McDonald, R. N.; Steppel, R. N.; Dorsey, J. E. *Org. Synth.* **1970**, *50*, 14.

(18) Schumb, W. F.; Satterfield, C. N.; Wentworth, R. L. *Hydrogen Peroxide*; Reinhold: New York, 1955; p 561.

(19) (a) Wilshire, J.; Sawer, D. T. *Acc. Chem. Res.* **1979**, *12*, 105. (b) Chin, D.-H.; Chiericato, G., Jr.; Nanni, E. J.; Sawer, D. T. *J. Am. Chem. Soc.* **1982**, *104*, 1296.

(20) Roberts, J. L.; Sawer, D. T. *J. Am. Chem. Soc.* **1981**, *103*, 712.

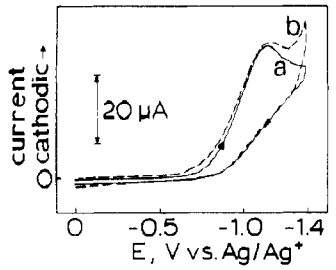

Figure 2. Cyclic voltammograms of oxygen reduction recorded at 0.1 V/s: curve a, at a naked GC electrode; curve b, at a GC electrode coated with poly-$[Ru(vbpy)_3]^{2+}$ (8.2×10^{-9} mol/cm^2), in 0.1 M Bu_4NClO_4–CH_2Cl_2 containing 0.1 M benzoic acid and 0.04 M 1-methylimidazole.

benzoic acid shifts the O_2 reduction potential positively, considerably at Pt electrodes and slightly at GC electrodes. The resulting O_2 reduction wave on Pt electrodes is not well-separated from that due to hydrogen evolution from the benzoic acid (curve b, upper), but the two processes are well-separated at GC electrodes because proton reduction there is kinetically slow (curve b, lower).

The efficiencies for electrolytic production of H_2O_2 by O_2 electrolysis at potentials suggested by the voltammograms in Figure 1 are shown in Table I. The analysis for H_2O_2 was performed as described in the Experimental Section. (Any possible production of perbenzoic acid by H_2O_2–benzoic acid reaction in the CH_2Cl_2 solution does not affect the H_2O_2 analysis, as shown by negative tests with synthetic perbenzoic solutions in CH_2Cl_2.) The H_2O_2 yield is quite poor at Pt electrodes (faradaic efficiency < 20%), and judging from the decrease in yield at more negative electrolysis potentials (Table I), the poor yield may be associated with further reduction of H_2O_2 and/or concurrent benzoic acid reduction (see curve b vs curve c, upper, Figure 1). The H_2O_2 yield, in contrast, is relatively large at the GC electrode, at potentials more positive than −1.4 V vs Ag/Ag^+ (curve b vs curve c, lower, Figure 1). The yields at the naked GC electrodes are, however, less than 100%.

Electrochemical Reduction of O_2 at Polymer-Coated Electrodes in Methylene Chloride. As long as relatively thin (<ca. 1×10^{-8} mol/cm^2) poly-$[Ru(vbpy)_3]^{2+}$ films are employed, the electroreduction of O_2 at coated GC electrodes (---, Figure 2) is little altered from that at naked (—) GC electrodes. The polymer film does not affect the electrode kinetics. Transport of O_2 to the electrode is slightly retarded by the requirement that the O_2 diffuse through the polymer film; evidence for this is given later. Most importantly, electrolysis producing H_2O_2 at poly-coated GC electrodes is, in contrast to that at naked GC electrodes, essentially quantitative (Table I). The quantitative yield is unaffected by addition of 1-methylimidazole. We are not certain about the reason for the quantitative yield of H_2O_2 at polymer-coated GC electrodes (relative to naked GC electrodes). It may be that the polymer film retards reactions between the superoxide intermediate and the solvent. The result is nonetheless an opportune one for the electrocatalytic experiments and for a simplified consideration of the reaction kinetics.

The H_2O_2 yield at the polymer-coated Pt electrode is again low (Table I), and little further work was performed with this electrode material.

Permeation of [Mn(TPP)Cl] through Poly-$[Ru(vbpy)]_3^{2+}$ Films. We have previously established[14] that electropolymerized metal polypyridine films act as molecular sieves, and so it was expected that poly-$[Ru(vbpy)_3]^{2+}$ films would act as effective transport barriers to the molecularly bulky porphyrins. This was confirmed by cyclic voltammograms such as those in Figure 3, where the $[Mn^{III/II}(TPP)Cl]$ reduction wave seen at a naked GC electrode (curve a) is nearly completely suppressed when the GC electrode is coated with a ~31-nm thick film of the polymer. Similar results are obtained on coated Pt electrodes.

The actual permeability of the poly-$[Ru(vbpy)_3]^{2+}$ film to [Mn(TPP)Cl] is best examined by using a rotated-disk experiment; results are shown in Figure 4. At the naked Pt electrode (curve a), the rotated-disk limiting current, i_l, for [Mn(TPP)Cl] reduction

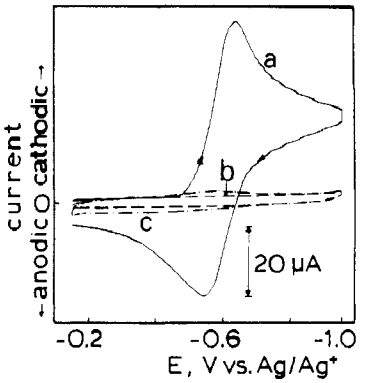

Figure 3. Cyclic voltammograms of 0.25 mM [Mn(TPP)Cl] in 0.1 M Bu_4NClO_4–CH_2Cl_2 at 0.1 V/s: curve a, at a naked GC electrode; curve b, at a GC electrode coated with poly-$[Ru(vbpy)_3]^{2+}$ (4.7×10^{-9} mol/cm^2); curve c, at the same electrode after use for an epoxidation electrolysis at −1.3 V vs Ag/Ag^+ at 900 rpm for 3 h.

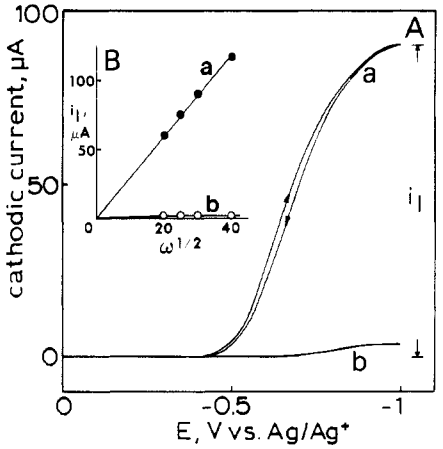

Figure 4. (A) Rotating-disk voltammograms of 0.32 mM [Mn(TPP)Cl] in 0.1 M Bu_4NClO_4–CH_2Cl_2 under Ar recorded at 900 rpm and 5 mV/s scan rate: curve a, at a naked Pt electrode; curve b, at a Pt electrode coated with 3.2×10^{-9} mol/cm^2 poly-$[Ru(vbpy)_3]^{2+}$. (B) Levich plot for limiting currents taken from voltammograms shown in A at a series of rotation rates.

varies linearly with the square root of electrode rotation rate, ω, but at the poly-$[Ru(vbpy)_3]^{2+}$-coated Pt electrode, i_l is much smaller (curve b, Figure 4) and less dependent on rotation rate. Analysis of the rotation rate data as previously described[14a] (Figure 4 inset) yields a polymer film permeability, $PD_{s,pol}$ (the product of the coefficients of partition into and diffusion in the polymer), of 9×10^{-10} cm^2/s. This permeability, under the conditions of an epoxidation electrolysis, translates into a current flow of 2 μA for the direct reduction of porphyrin by transport through the polymer film barrier. This current is only ca. 1% of the typical oxygen reduction current observed in the epoxidation electrolyses (see Table IV), which means the requirements of Scheme I for avoiding direct electron transfer between electrode and porphyrin are amply satisfied. We assume that the permeability of the polymer to the oxo porphyrin is similar to that of [Mn(TPP)Cl] and also note that the poly-$[Ru(vbpy)_3]^{2+}$ polymer is not electroactive in the potential range used for the O_2 electrolyses, a necessary characteristic for the polymer to act as a mass-transport barrier. That is, the polymer film does not act as an electron-transfer mediator for the porphyrin.

The poly-$[Ru(vbpy)_3]^{2+}$ films are furthermore quite durable under electrolysis conditions (even when the electrode is constantly rotated). This is illustrated by the curve b,c comparison in Figure 3, which shows that the suppression of [Mn(TPP)Cl] reduction by a poly-$[Ru(vbpy)_3]^{2+}$ film is unchanged after being used in a 3-h epoxidation electrolysis.

Epoxidation Results. Results for the production of epoxide using polymer-coated electrodes in Scheme I are given in Tables II–VI and Figures 5–7. Figures 5–7 show respectively how the rate

Table II. Electrochemical Olefin Epoxidation[a]

run	electrode; potential, V; time, h[b]	[Mn(TPP)Cl] concn, mM	other conditions	i_c,[c] mA	[epoxide],[d] mM CO	[epoxide],[d] mM TO	faradaic efficiency, %	turnovers	[Mn(TPP)Cl] recovery, %
			0.05 M Cyclooctene and 0.05 M *trans*-2-Octene						
1	Pt; −0.9; 3	0.1	*e*	0.35	0.83	*f*	0	8.3	95
2	Pt/poly; −0.9; 3	0.1	*e*	0.06	0.21	t	12	2.1	100
3	GC; −1.3; 3	0.1	*g*	1.02	0.30	t	1	3.0	85
4	GC; −1.3; 3	0.1		1.33	3.3	0.24	9	35	95
5	GC/poly; −1.3; 3	0.1		0.89	6.3	0.40	27	67	90
6	GC; −1.3; 3	1.0		1.42	3.3	0.28	7	3.6	100
7	GC/poly; −1.3; 3	1.0		0.63	7.1	0.53	43	7.6	100
			0.4 M Cyclooctene						
8	GC; −1.3; 1	0.2		0.99	4.4		48	22	100
9	GC/poly; −1.3; 1	0.2		0.47	4.2		96	21	100
10	GC/poly; −1.0; 1	0.2		0.15	5.3		94	25	100
11	GC/poly; −1.0; 4	0		0.15	0.01		1		
			0.1 M Cyclooctene						
12	GC/poly; −1.3; 1	0.1	*h*	0.34	t		0	0	1
13	GC/poly; −1.3; 1	0.1	*i*	0.63	0.22		4	2	3

[a] Electrolysis at a rotated (900 rpm) disk electrode in 2 mL of 0.1 M Bu_4NClO_4–CH_2Cl_2 containing [Mn(TPP)Cl], indicated olefin, 0.1 M benzoic acid, 0.04 M 1-methylimidazole, and decane, except as stated under "other conditions". Rotated electrode was either naked Pt or glassy carbon (GC), or these materials coated with (3–5) × 10^{-9} mol/cm^2 poly-$[Ru(vbpy)_3]^{2+}$. [b] Electrode is naked or polymer-coated as indicated; potential is electrolysis potential vs Ag/Ag^+; time is electrolysis time. [c] Steady-state electrolysis current. [d] CO = cyclooctene oxide; TO = *trans*-2-octene oxide. [e] 0.2 M 1-methylimidazole. [f] Trace (<0.05 mM). [g] No 1-methylimidazole. [h] No benzoic acid. [i] No benzoic acid; 0.16 M $Bu_4N(OCOPh)$.

Table III. Epoxidation by Direct Addition of Oxygenating Agents

run	system	addn method	[epoxide],[a] mM CO	[epoxide],[a] mM TO	yield per ROOH, %	recovery of [Mn(TPP)Cl], %
		Solution A[b]				
1	H_2O_2 (274)	slow	1.1	0	4	0
2	H_2O_2 (276) + 0.1 M $Bu_4N(OCOPh)$	slow	0.6	0	2	0
3	H_2O_2 (276) + 0.1 M PhCOOH	slow	159	11	62	55
4	H_2O_2 (276) + PhCOOH	rapid	94	4	35	0
5	$PhCO_3H$ (280)	rapid	246	21	95	36
		Solution B[c]				
6	H_2O_2 (60) + 0.1 M PhCOOH	slow	54		90	80
7	H_2O_2 (60) + 0.1 M PhCOOH	slow	51		85	85

[a] CO = cyclooctene oxide; TO = *trans*-2-octene oxide. [b] Solution A: The chemicals indicated, in 2 mL of 1:1 CH_2Cl_2–CH_3CN, were added, slowly or rapidly as indicated, with magnetic stirring to 2 mL of a CH_2Cl_2 solution containing 0.1 mM [Mn(TPP)Cl], 0.05 M cyclooctene, 0.05 M *trans*-2-octene, and 0.04 M 1-methylimidazole. The notation H_2O_2 (274) means an excess of 274 equiv of H_2O_2/equiv of [Mn(TPP)Cl]. In run 4, H_2O_2 and benzoic acid were first incubated together in CH_2Cl_2–CH_3CN solution for 2 h. [c] Solution B: A 1:9 mixture of 30% aqueous H_2O_2–CH_3CN was added to 2 mL of a 0.1 M Bu_4NClO_4–CH_2Cl_2 solution containing 0.2 mM [Mn(TPP)Cl], 0.4 M cyclooctene, and 0.1 M benzoic acid, in which a 3.6 × 10^{-9} mol/cm^2 poly-$[Ru(vbpy)_3]^{2+}$-coated glass-carbon electrode was rotating at 900 rpm under Ar. In run 6 the electrode was disconnected; its potential was −1.3 V vs Ag/Ag^+ in run 7. The notation H_2O_2 (60) means an excess of 60 equiv of H_2O_2/equiv of [Mn(TPP)Cl].

Table IV. Electrochemical Epoxidation at Poly-$[Ru(vbpy)_3]^{2+}$-Coated Glassy-Carbon Electrodes

	electropolymerization[a]			epoxidation[b]			
run	[monomer], mM	no. of cyclic scans	$10^9\Gamma$, mol/cm^2	*E*, V vs Ag/Ag^+	i_c, mA	[CO], mM	faradaic efficiency, %
1	0.1	60	2.6	−1.15	0.20	1.65	88
2	0.1	75	2.8	−1.15	0.22	1.84	91
3	0.1	60	3.0	−1.15	0.16	1.34	92
4	0.1	80	2.3	−1.3	0.40	3.67	98
5	0.1	40	2.4	−1.3	0.47	4.22	96
6	0.3	10	3.9	−1.0	0.15	1.21	86
7	0.3	10	2.8	−1.15	0.18	1.58	96
8	0.3	15	3.6	−1.3	0.20	1.64	89
9	0.5	7	3.0	−1.3	0.47	3.74	86
10	0.5	5	3.2	−1.3	0.46	4.07	95

[a] See the Experimental Section. [b] Epoxidation electrolysis was carried out at a poly-$[Ru(vbpy)_3]^{2+}$-coated disk electrode rotating at 900 rpm for 1 h in 0.1 M Bu_4NClO_4–CH_2Cl with 0.2 mM [Mn(TPP)Cl, 0.4 M cyclooctene, 0.1 M benzoic acid, 0.04 M 1-methylimidazole, and decane. The product of current i_c and time vs the concentration of epoxide-produced [CO] gives faradaic efficiency.

Table V. Dependency of Faradaic Efficiency of Epoxidation on Electrode Potential and Rotation Rate

electrolysis conditions[a]	*E*, V vs Ag/Ag^+	ω, rpm	i_c, mA	[CO], mM	faradaic efficiency, %
	0.1 mM [Mn(TPP)Cl] and 0.1 M Cyclooctene				
A	−1.0	900	0.17	1.22	79
A	−1.1	900	0.25	1.77	77
A	−1.2	900	0.39	2.90	80
A	−1.3	900	0.54	4.45	88
	0.2 mM [Mn(TPP)Cl] and 0.4 M Cyclooctene				
B	−1.15	400	0.17	1.42	89
B	−1.15	900	0.18	1.58	96
B	−1.15	1600	0.23	2.11	97

[a] Electrolysis was carried out at a 2.8 × 10^{-9} mol/cm^2 poly-$[Ru(bpy)_3]^{2+}$-coated glassy-carbon electrode in 0.1 M Bu_4NClO_4–CH_2Cl_2 containing 0.1 M benzoic acid, 0.04 M 1-methylimidazole, and decane for 1 h.

of epoxide production depends on reaction time at various concentrations of the reagents, on the olefin concentration, and on the porphyrin catalyst concentration. Tables II and IV–VI give numerical reaction yield, stability, and other data on respectively reactions under a variety of conditions, reproducibility of the reaction, reaction dependency on electrode potential and rotation rate, and porphyrin and olefin concentration dependency for [Mn(TPP)Cl], [Mn(TMP)Cl], and [Mn(TF_5PP)Cl] catalysts. Table III gives results for direct (as opposed to electrochemical) addition of H_2O_2 to olefin solutions. The following discussion draws from this collection of results.

Yield and Stability. The essential aspect of Scheme I is that H_2O_2 is produced electrochemically, generating the reactive oxo porphyrin [Mn(=O)(TPP)], which reacts with olefin and is

Table VI. Epoxidation Yields for Mn Porphyrins[a]

porphyrin	[porphyrin], mM	[cyclooctene], M	faradaic efficiency, %	recovery of porphyrin, %
[Mn(TPP)Cl]	0.2	0.4	92 ± 4	100
[Mn(TPP)Cl]	0.002	0.4	7 ± 3	0
[Mn(TPP)Cl]	0.1	0.01	29	100
[Mn(TMP)Cl]	0.2	0.4	64 ± 1	100
[Mn(TMP)Cl]	0.002	0.4	6 ± 4	55
[Mn(TMP)Cl]	0.1	0.01	13 ± 2	90
[Mn(TF_5PP)Cl]	0.2	0.4	39 ● 10	100
[Mn(TF_5PP)Cl]	0.002	0.4	41 ± 21	40
[Mn(TF_5PP)Cl]	0.1	0.01	7 ± 3	100

[a] Electrolysis was carried out at 2–4 × 10^{-9} mol/cm² poly-[Ru(vbpy)$_3$]$^{2+}$-coated glassy-carbon electrodes rotating at 900 rpm at −1.0 or −1.15 V vs Ag/Ag$^+$ for 1 h in 0.1 M Bu_4NClO_4–CH_2Cl_2 containing 0.1 M benzoic acid, 0.04 M 1-methylimidazole, and decane. Currents were in the range 0.14–0.23 mA.

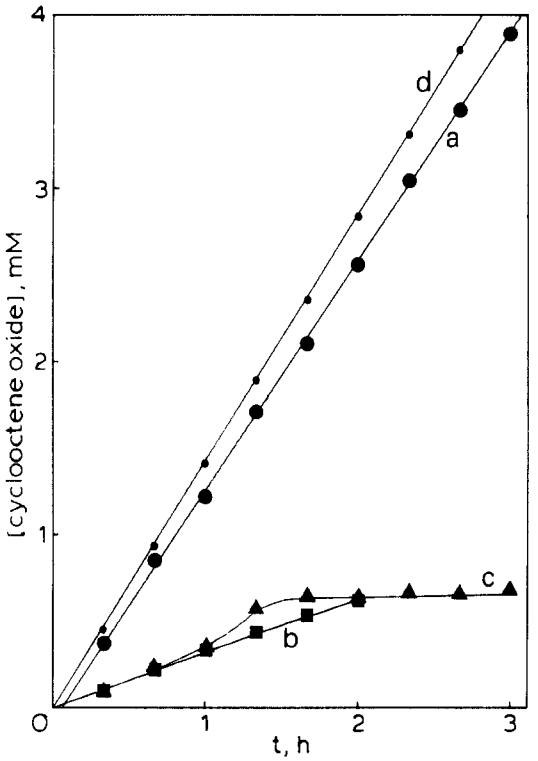

Figure 5. Cyclooctene oxide production vs time in controlled-potential epoxidation electrolysis at −1.0 V vs Ag/Ag$^+$ at a GC electrode coated with poly-[Ru(vbpy)$_3$]$^{2+}$ (3.9 × 10^{-9} mol/cm²) rotating at 900 rpm in 0.1 M Bu_4NClO_4–CH_2Cl_2 containing [Mn(TPP)Cl], cyclooctene, 0.1 M benzoic acid, 0.04 M 1-methylimidazole, and decane: curve a, 0.21 mM [Mn(TPP)Cl], 0.40 M cyclooctene; curve b, 0.10 mM [Mn(TPP)Cl], 0.0051 M cyclooctene; curve c, 0.0064 mM [Mn(TPP)Cl], 0.40 M cyclooctene; curve d, theoretical curve for 100% faradaic efficiency in curve a.

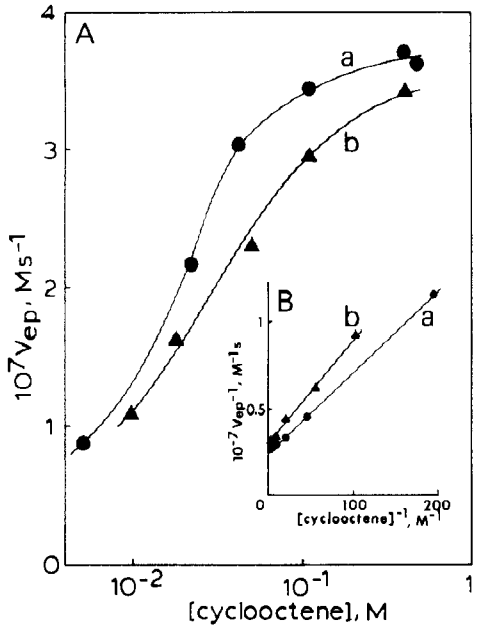

Figure 6. (A) Epoxidation rate, mol/s, vs cyclooctene concentration in the controlled-potential electrolysis at a GC electrode coated with poly-[Ru(vbpy)$_3$]$^{2+}$ rotating at 900 rpm in 0.1 M Bu_4NClO_4–CH_2Cl_2 containing 0.1 mM [Mn(TPP)Cl], 0.1 M benzoic acid, and 0.04 M 1-methylimidazole: curve a, 3.9 × 10^{-9} mol/cm² polymer, current 0.167 ± 0.008 mA; curve b, 3.0 × 10^{-9} mol/cm² polymer, current 0.142 ± 0.010 mA. (B) Double-reciprocal plots of the data plotted in part A.

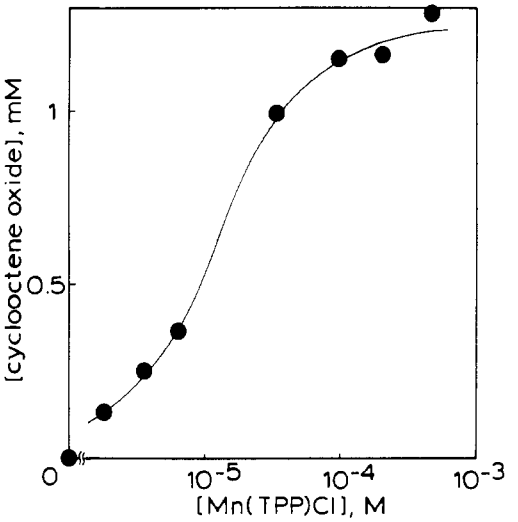

Figure 7. Cyclooctene oxide production vs initial [Mn(TPP)Cl] concentration in controlled-potential electrolysis at a GC electrode coated with poly-[Ru(vbpy)$_3$]$^{2+}$ (3.9 × 10^{-9} mol/cm²) rotating at 900 rpm in 0.1 M Bu_4NClO_4–CH_2Cl_2 containing 0.4 M cyclooctene, 0.1 M benzoic acid, 0.04 M 1-methylimidazole, and decane for 1 h.

prevented from unproductive electroreduction by the polymer film mass-transport barrier. Results shown in Table II demonstrate the efficacy of this tactic, as can be seen by comparison of the faradaic efficiency results for naked vs coated electrodes in runs 4 vs 5, 6 vs 7, and 8 vs 9. Faradaic efficiency is the percentage of epoxide produced (as given by the GC electrode analysis and assuming two electrons per epoxide) as compared to the electrochemical charge passed during the electrolysis (the product of the electrolysis current i_c and electrolysis time), that is, the efficiency in use of the electrochemical reducing equivalents. In every comparison, much higher efficiencies are observed with the polymer film present. The results show, indirectly, that the electroreduction of the oxo porphyrin is suppressed by the polymer-transport barrier. The results also indicate that reduction of [Mn^{III}(TPP)Cl] is suppressed, since such reduction would mediate [Mn(=O)(TPP)] reduction and cause lower efficiency. The results in Table IV also show that efficiency does not depend on details of the electropolymerization preparation of the polymer coating.

The highest faradaic efficiencies found in the results shown in Tables II and IV–VI are those at the higher olefin and [Mn(TPP)Cl] concentrations. These efficiencies are near-quantitative, in fact, in the 80 to upper 90% range. Figure 5, curve a, is nearly coincident with the theoretical 100% efficiency, curve d, and also shows by its linearity that this high efficiency can be maintained over at least a 3-h electrolysis. These results indicate that the H_2O_2 electrode reaction product is most effectively utilized under conditions where buildup of excess H_2O_2 or of [Mn(=O)(TPP)] is minimized. In our previous[12] electrocatalytic epoxidation studies, results were seen that were consistent with loss of oxo porphyrin by electroreduction at uncoated electrodes; the present results substantiate those observations.

When low concentrations of porphyrin catalyst or olefin are employed, on the other hand, noticeably lower faradaic efficiencies

are observed (Table II, runs 5 and 7, and Table VI). While the polymer coating appears effective at suppressing porphyrin reactions as a source of reaction inefficiency, there appear to be at least two other side reactions that become important under low-concentration conditions. One side reaction is revealed, in general form at least, by the data on recovery of the porphyrin catalyst. At high porphyrin and olefin concentrations, the porphyrin is recovered at levels typically in the 90–100% range (as tested by spectrophotometric analysis) following completion of the electrolysis. Under these conditions, then, the reaction seems remarkably stable, especially given the notoriety of H_2O_2 as a destroyer of porphyrins, the oxidative reactivity of metal oxo porphyrin, and the use of an "unprotected" porphyrin. In contrast, at low porphyrin concentrations, the percent recovery of porphyrin drops sharply (see results for 0.002 mM porphyrin in Table VI). Comparison of curve c to curve d in Figure 5 shows an efficiency less than 100% at short electrolysis times, followed by a leveling off of epoxide production. This occurs because, as seen by spectrophotometric analysis, the porphyrin has been degraded, presumably by reaction with H_2O_2 when the latter is in persistent excess.

While electrolysis efficiency is low at low olefin concentrations (compare curves b and d, Figure 5), this does not seem to involve porphyrin degradation (see Table II, runs 1–7, and Table VI). A second pathway to consume electrochemical reducing equivalents appears to exist. We can only speculate as to what this may be, but at least one possibility is a catalase-like reaction between H_2O_2 and oxo porphyrin[21]

$$[Mn(=O)(TPP)] + H_2O_2 \rightarrow [Mn^{III}TPP] + O_2 + H_2O \quad (1)$$

Such a reaction would be most important, in a competitive kinetic sense, at low olefin concentration.

Stereoselectivity, Kinetics, and Mechanism. High regioselectivity is an important aspect of metalloporphyrin-based epoxidations. Competition kinetics between cis and trans olefin substrates is a useful criterion for oxo metalloporphyrin vs other reaction pathways. In competition experiments using 1:1 mixtures of cyclooctene and *trans*-2-octene, the cis:trans selectivity was 14:1 when H_2O_2 was added directly to [Mn(TPP)Cl]–PhCOOH–olefin mixtures (Table III, run 3), 12:1 similarly when $PhCO_3H$ was used (Table III, run 5), 15:1 when PhIO was used with [Mn(TPP)Cl],[12a] and 4:1 when epoxidation was completed with 2-chloroperoxybenzoic acid.[12a] The electrochemical epoxidation gave cis:trans selectivities of (12–16):1 (Table II, runs 4–7), similar to the PhIO and direct H_2O_2 addition results, with complete recovery of porphyrin catalyst as measured spectrophotometrically.

The dependency of the electrochemical epoxidation on olefin concentration (at high porphyrin concentration) and on porphyrin concentration (at high olefin concentration) is shown in Figures 6 and 7, respectively. In both sets of experiments the reaction rate saturates at high concentration. The value of the saturated epoxidation rate is sensitive to electrochemical parameters that (at constant reagent concentration) accelerate the production of H_2O_2. This is seen in Tables IV and V in that use of the more negative electrolysis potentials (shown by the data in Table I to cause a faster rate of production of H_2O_2) results in faster epoxidation rates. Use of faster electrode rotation rates also causes faster epoxidation (Table V). The rates do not increase in a Levich fashion (with square root of rotation rate) because the polymer membrane offers some transport impedance to the O_2 substrate. From these observations we believe then that the saturation in rate is determined by the overall velocity of electrochemical H_2O_2 production, i.e.

$$O_2 + 2H^+ + 2e^- \xrightarrow{V_2} H_2O_2 \quad (2)$$

This point is pertinent to possible preparative aspects of Scheme I; factors known to increase electrolysis rate (electrode area, mass-transport rate, dioxygen concentration) should enhance the saturation reaction velocity for epoxide production. We have not emphasized such tactics here.

Figures 6 and 7 show that the epoxidation rate diminishes at lower olefin and porphyrin concentrations. These rate effects are qualitatively expected, from previous investigations of epoxidation kinetics with analogous systems[4,22,23] for diminution of the rate of oxo porphyrin formation

$$Mn(por) + H_2O_2 \cdots (por)Mn(H_2O_2) \rightarrow [(por)Mn{=}O]^+ + H_2O \quad (3)$$

at low porphyrin concentration and for decrease in formation of oxo–porphyrin–olefin complex

$$[(por)Mn{=}O]^+ + \text{olefin} \underset{}{\overset{K_m}{\rightleftharpoons}} [(por)Mn{=}O(\text{olefin})]^+ \xrightarrow{V_{max}} Mn(por) + \text{epoxide} \quad (4)$$

at low olefin concentration. Analysis of the reaction kinetics is complicated in the present data, however, because of (a) onset of kinetic control of reaction 2 at high concentrations, (b) lower faradaic efficiencies at low concentrations of both olefin and porphyrin, and (c) degradation of porphyrin when its concentration is low. The inset in Figure 6 shows an attempted analysis of the olefin concentration dependency using the equation[4,24]

$$V_{epox}^{-1} = V_2^{-1} + V_4^{-1} = K_m/(V_{max}[\text{olefin}]) + V_2^{-1} + V_{max}^{-1} \quad (5)$$

which assumes that, at high porphyrin concentration, the rate control is by reactions 2 and 4. From the discussion above we expect that reaction 2 controls the intercept of the plot. A value of $K_m/V_{max} = 5.3\ (+0.6) \times 10^4$ s was obtained from the slope, which is larger than the value of 50 s obtained in the hypochlorite oxygenation system.[25] This discrepancy is probably a reflection simply of the catalase-like side reaction (1) which, because it has a relatively greater effect at low olefin concentration, would artificially act to elevate the K_m/V_{max} result.[26] Such effects by competitive reactions have been mentioned for a solution with two kinds of olefins.[27]

We should note a number of control experiments that add evidence for Scheme I and the proposed role of oxo porphyrin in the epoxidation (reaction 4). First, the results given in Table II, where 1-methylimidazole (run 3), [Mn(TPP)Cl] (run 11), and benzoic acid (run 12) are omitted show their essential participation in the scheme. Second, perbenzoic acid formation from H_2O_2 and benzoic acid should be minor because the reaction medium is not strongly acidic.[28] This was confirmed by the quantitative stoichiometry of the electrolytic formation of H_2O_2 demonstrated at the polymer-coated carbon electrode (Table I), plus the observation that perbenzoic acid does not register in the H_2O_2 assay. Table III, runs 5 and 6, further shows that the efficiency of a reaction using H_2O_2 incubated with benzoic acid (Table III, run 6) and of one using perbenzoic acid (run 5) are not the same, the latter actually being higher than for H_2O_2. Third, the nonelectro-

(21) Schonbaum, G. R.; Chance, B. In *The Enzymes*, 3rd ed.; Boyer, P. D., Ed.; Academic Press: New York, 1976; Vol. 13, p 363.

(22) (a) Zipplies, M. F.; Lee, W. A.; Bruice, T. C. *J. Am. Chem. Soc.* **1986**, *108*, 4433. (b) Balasubramanian, P. N.; Schmidt, E. S.; Bruice, T. C. *Ibid.* **1987**, *109*, 7865.

(23) Traylor, T. G.; Xu, F. *J. Am. Chem. Soc.* **1988**, *110*, 1953.

(24) Lineweaver, H.; Burk, D. *J. Am. Chem. Soc.* **1934**, *56*, 658.

(25) In the hypochlorite oxygenation system, K_m/V_{max} for [Mn(TMP)Cl]–cyclooctene is 50 s.[4b] [Mn(TPP)Cl] should not have a value larger than 50 s because the dependency of the epoxidation rate on [Mn(TPP)Cl] concentration is smaller than that on [Mn(TMP)Cl].[4b]

(26) It has been recently reported that a dimer conproportionation between Mn(III) porphyrin and Mn(V) oxo porphyrin exists in some porphyrin reactions: Lee, R. W.; Nakagaki, P. C.; Bruice, T. C. *J. Am. Chem. Soc.* **1989**, *111*, 1368. At high olefin concentration, where the concentration of oxo porphyrin is low, effects of such conproportionation should be negligible. At low olefin concentration conproportionation is competitive to reaction 4 and may increase the apparent K_m/V_{max} as the catalase-like reaction does. Our data give no information on the occurrence of this conproportionation or on its associated kinetics.

(27) Tulinsky, A.; Chen, B. M. L. *J. Am. Chem. Soc.* **1977**, *99*, 3647.

(28) Silvert, L. S.; Siegel, E.; Swern, D. *J. Org. Chem.* **1962**, *27*, 1336.

chemical results in Table III, runs 1 and 2 vs run 3, show that benzoic acid must play a second role, besides as a proton source in the electrochemical formation (reaction 2) of H_2O_2, by either promoting the formation of the oxo porphyrin (reaction 3) or the epoxidation rate or oxo-porphyrin-olefin complex stability (reaction 4). Similar effects of acid-base combinations (buffers) have been reported in iron porphyrin-hydrogen peroxide reactions.[22a] Porphyrin degradation is extensive in the absence of the acid, and benzoate alone, as potential axial ligand, is insufficient (run 2).

Finally, we consider the epoxide yield and porphyrin stability results in Table VI, where the "protected" porphyrins are compared to [Mn(TPP)Cl]. As expected, these porphyrins were more resistant to degradation when used at low concentrations. Some decomposition does occur, however. It is noteworthy that [Mn(TF_5PP)Cl] gives a much higher yield at a low catalyst concentration than other porphyrins. This means a fast reaction step (4), which is consistent with high turnovers of F-substituted derivatives of manganese and iron tetraphenylporphyrin.[29] In addition, the faradaic efficiency of the electrolysis was lower with the protected porphyrins than with [Mn(TPP)Cl]. It may be that the competing catalase reaction (1) is more important for these materials.

Acknowledgment. This research was supported in part by grants from the NSF (R.W.M.) and NIH (J.P.C., Grant 5 RO1 GM17880). H.N. expresses gratitude for sabbatical leave support from the Yozaki Memorial Foundation for Science and Technology and from Keio University, Yokohama, Japan.

(29) Takagi, S.; Takahashi, E.; Miyamoto, T. K.; Sasaki, Y. *Chem. Lett.* **1986**, 1275.

Contribution from the Departments of Chemistry, Rensselaer Polytechnic Institute, Troy, New York 12180, and The University of North Carolina at Chapel Hill, Chapel Hill, North Carolina 27599-3290

Electrocatalytic Olefin Epoxidation Using Manganese Schiff-Base Complexes and Dioxygen

Colin P. Horwitz,*[1,2] Stephen E. Creager,[3] and Royce W. Murray*[3]

Received February 14, 1989

Electrochemical reduction of $[Mn^{III}(salen)]^+$ (salen = *N,N'*-ethylenebis(salicylaldiminato)) complexes in acetonitrile solution in the presence of benzoic anhydride, 1-methylimidazole, dioxygen, and an olefin yields the epoxide of the olefin in as much as 48% yield based on electrochemical charge passed. Cyclic voltammetric and rotating-disk voltammetric results are consistent with an electron/dioxygen bonding/electron (ECE) reaction sequence to produce a manganese-peroxo complex in which the O-O bond is subsequently heterolyzed by reaction with benzoic anhydride to yield a Mn(V)-oxo complex. Cis/trans kinetic competition experiments with *cis*-cyclooctene and *trans*-2-octene give a cis/trans reactivity ratio of 10 for the electrolytic epoxidation. Iodosylbenzene gives a ratio of 14 under comparable conditions. Electrolysis in the presence of cyclohexene yields primarily cyclohexene oxide and significant quantities of the allylic oxidation products 2-cyclohexen-1-one and 2-cyclohexen-1-ol.

The homogeneous catalytic transformation of organic substrates by transition-metal compounds is an area of intense research activity. This interest arises from the possibilities of improving existing or discovering new catalytic reactions and from the biological relevance of transition-metal compounds to active sites of various enzymes. There is also interest in using electrochemical techniques[4] in conjunction with metal complex catalysts. We recently used[5] a manganese porphyrin as an electrocatalyst in the reductive activation of dioxygen toward olefin epoxidation in a scheme considered as a model reaction for the cytochrome P450 class of monooxygenase enzymes

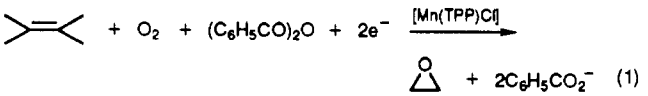

(1)

where Mn(TPP) is manganese(III) tetraphenylporphyrin and $(C_6H_5CO)_2O$ is benzoic anhydride.

Olefin epoxidation reactions have been extensively investigated[6] with manganese porphyrin catalysts, in which an activated form of oxygen, such as iodosylbenzene, is employed as the oxygen source (eq 2). The analogous reaction with manganese Schiff-base

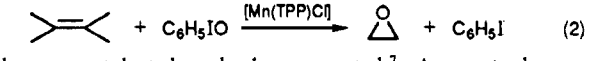

(2)

complexes as catalysts has also been reported.[7] A recent advance in this area[8] is olefin epoxidation using nickel Schiff-base and related complexes under phase-transfer conditions with NaOCl as the oxygen source. The nickel complexes are poor epoxidation catalysts when iodosylbenzene replaces hypochlorite.[8,9]

The necessity for the "preactivation" of dioxygen in the form of iodosylbenzene or hypochlorite is a potential disadvantage

(1) Rensselaer Polytechnic Institute.
(2) Work done at The University of North Carolina at Chapel Hill.
(3) The University of North Carolina at Chapel Hill.
(4) (a) See for example: Steckhan, E. *Angew. Chem., Int. Ed. Engl.* **1986**, *25*, 683. (b) *Organic Electrochemistry*; Baizer, M. M.; Lund, H., Eds.; Marcel Dekker: New York, 1983. (c) Scheffold, R.; Rytz, G.; Walder, L.; Orlinski, R.; Chilmonczyk, Z. *Pure Appl. Chem.* **1983**, *55*, 1791. (d) Collman, J. P.; Denisevich, P.; Konai, Y.; Marrocco, E.; Koval, C.; Anson, F. C. *J. Am. Chem. Soc.* **1980**, *102*, 6027.
(5) Creager, S. E.; Raybuck, S. A.; Murray, R. W. *J. Am. Chem. Soc.* **1986**, *108*, 4225.
(6) (a) See for example: Tabushi, I. *Coord. Chem. Rev.* **1988**, *86*, 1. (b) Castellino, A. J.; Bruice, T. C. *J. Am. Chem. Soc.* **1988**, *110*, 158. (c) Groves, J. T.; Stern, M. K. *Ibid.* **1987**, *109*, 3812. (d) Groves, J. T.; Watanabe, Y.; McMurry, T. J. *Ibid.* **1983**, *105*, 4489. (e) Collman, J. P.; Brauman, J. I.; Meunier, B.; Hayashi, T.; Kodadek, T.; Raybuck, S. A. *Ibid.* **1985**, *107*, 2000. (f) Smegal, J. A.; Schardt, B. C.; Hill, C. L. *Ibid.* **1983**, *105*, 3510. (g) Guilmet, E.; Meunier, B. *Tetrahedron Lett.* **1982**, 2449. (h) Carvalho, M. E.; Meunier, B. *Nouv. J. Chim.* **1986**, *10*, 39.
(7) (a) Srinivasan, K.; Michaud, P.; Kochi, J. K. *J. Am. Chem. Soc.* **1986**, *108*, 2309. (b) Dixit, P. S.; Srinivasan, K. *Inorg. Chem.* **1988**, *27*, 4507. (c) Srinivasan, K.; Perrier, S.; Kochi, J. K. *J. Mol. Catal.* **1986**, *36*, 297.
(8) (a) Yoon, H.; Burrows, C. J. *J. Am. Chem. Soc.* **1988**, *110*, 4087. (b) Kinneary, J. F.; Albert, J. S.; Burrows, C. J. *Ibid.* **1988**, *110*, 6124.
(9) Koola, J. D.; Kochi, J. K. *Inorg. Chem.* **1987**, *26*, 908.

0020-1669/90/1329-1006$02.50/0